A Framework for The Optimal k-Coverage Deployment Patterns of Wireless Sensor Networks

Kazuya Sakai, *Member, IEEE,* Min-Te Sun, *Member, IEEE,* Wei-Shinn Ku, *Senior Member, IEEE,* and Ten H. Lai, *Senior Member, IEEE* Athanasios V. Vasilakos, *Senior Member, IEEE*

Abstract—The strategy for node deployment to achieve multiple connectivity and coverage plays an important role in various wireless network applications. To alleviate the operational cost, the number of nodes to be deployed needs to be reduced. While the optimal k-connectivity deployment patterns ($k \leq 6$) and the multiple k-coverage problem ($k \leq 3$) have been extensively studied for 2-D networks, a general method to identify the optimal deployment pattern for any given coverage requirement has yet to be found. Considering the ease of node deployment and operation, the deployment patterns should be identical and symmetric in the deployment region. This implies that the Voronoi diagram of the optimal deployment is a regular tessellation. Based on the fact that there exist only three regular tessellations, we propose a framework, namely Range Elimination Scheme (RES), to compute the optimal k-coverage deployment pattern for any given k value to accommodate various wireless application requirements. We apply RES to show the optimal k-coverage deployment patterns for $4 \leq k \leq 9$. Our analytical and simulation results show that our proposed framework successfully identifies the optimal deployment patterns and significantly reduces the number of nodes to be deployed.

Index Terms—Wireless sensor network topology, Optimal deployment pattern, Coverage

1 Introduction

Node deployment pattern is of great importance for many applications of wireless networks, such as activity sensing [1], monitoring [2], [3], RFID tracking [4], localization [5], and topology control [6]. In these applications, a large number of sensor nodes or RFID tags are deployed in the field with a regular pattern. The square pattern is commonly used, since it is the most intuitive and the easiest pattern for deployment. However, the hardware cost will be significantly lowered if the number of deployed nodes can be minimized under a certain set of coverage and connectivity requirements.

In [7], it is shown that an equilateral triangle with the nearest neighbors' distance $\sqrt{3}r$, where r is the radius of the circle that a node can cover, is the optimal single coverage deployment pattern. Recently, Zhang and Hou [1] proved the optimality of the equilateral triangle with $\sqrt{3}r$ for full coverage in a different way. When it comes to wireless networks, it is also important to consider the connectivity of nodes for fault tolerance. In [8]–[11], Bai *et al.* proposed the optimal deployment patterns for full-coverage and k-connectivity ($k \leq 6$) for various ratios between the sensing range and communication range. k-connectivity means that a graph is still connected even if arbitrary $k - 1$ nodes are removed. In addition to 2-D deployment patterns, 3-D patterns are investigated in [12]–[14].

While k-connectivity deployment patterns are well studied, little has been done for k-coverage deployment patterns. The k-coverage problem is defined as finding a deployment pattern such that every point in the region is covered by at least k nodes. The k-coverage deployment has applications on sensor/RFID localization, and thus this problem is both theoretically and practically significant. While Ku *et al.* [5] proved that the hexagon pattern with r and the equilateral triangle with r are the optimal patterns for $k = 2, 3$, respectively, the optimal k-coverage deployment patterns for $k \geq 4$ have yet to be identified. Since the effect of the boundary is very small when the deployment area is large, we do not consider the shape of the boundary. Therefore, in the rest of this paper, we refer to *optimal* as *asymptotic optimal*.

In this paper, a framework for finding the optimal k-coverage deployment patterns for arbitrary k values is proposed. First, we define the Voronoi region (i.e., tessella) of a node. Due to the simplicity of deployment and requirements from applications, the Voronoi region of each node should be identical and symmetric. We then convert the problem of optimal k-coverage deployment patterns into regular tessellations for a 2-D plane. Since there exist only three regular tessellations for a 2-D plane, *triangle*, *square*, and *hexagon*, it implies that the optimal k-coverage deployment patterns for an arbitrary k value can be obtained by simply checking a few cases. Based on this concept, we propose a framework, namely

Kazuya Sakai is with the Department of Information and Communication Systems, Tokyo Metropolitan University, 6-6 Asahigaoka, Hino-shi, Tokyo 191-0065, Japan. Email: ksakai@tmu.ac.jp
Min-Te Sun is with the Department of Computer Science and Information Engineering, National Central University, Taoyuan 320, Taiwan. E-mail: msun@csie.ncu.edu.tw
Wei-Shinn Ku is with the Department of Computer Science and Software Engineering, Auburn University, Auburn, AL 36849, USA. E-mail: weishinn@auburn.edu
Ten H. Lai is with the Department of Computer Science and Engineering, The Ohio State University, Columbus, OH 43210, USA. E-mail: lai@cse.ohio-state.edu
Athanasios V. Vasilakos is with the Department of Computer and Telecommunications Engineering, University of Western Macedonia, Parko Agiou Dimitriou, GR 50100 Kozani, Greece. E-mail:vasilako@ath.forthnet.gr

Range Elimination Scheme (RES), which finds the optimal k-coverage deployment pattern for any given k value. In RES, nodes are trimmed down to a small candidate set by a simple rule. Afterwards, the $(k-1)$-coverage deployment patterns are utilized to reduce the search space for the optimal k-coverage deployment pattern. As an example, we demonstrate how RES works for $4 \leq k \leq 9$.

The motivations for high k values, the novelty of this paper, and the paper organization are elaborated on the subsequent sections.

1.1 Motivations for High k Values

Higher connectivity and coverage are crucial in constructing an invulnerable and reliable wireless application. To achieve such requirements, a large number of nodes have to be deployed, which in turn results in high operational costs. Consequently, finding an efficient deployment strategy which minimizes the number of nodes to be deployed is of great significance from both theoretical and practical aspects. While the optimal k-coverage deployment patterns for $k \leq 3$ have been discovered in [1], [5], to the best of our knowledge a general method to identify the optimal k-coverage deployment pattern for any k value has yet to be found.

In addition, some wireless applications require very high coverage condition. For example, an electronic-and-vision surveillance system [3] is one of them. In a target area, such as an airport, a military base, etc., many camera sensors are placed to detect and monitor everyone there. However, it is common that one camera targets at one person within its sensing area at a time. With the 9-coverage deployment, up to 9 suspicious people can be monitored. In a critical area, such as the university campus in a day that President provides a speech, the coverage requirement becomes extremely high for the President protection. In other words, the value of k should be as large as possible.

Therefore, we are motivated to develop a framework which helps identify the optimal k-coverage deployment patterns for large k values.

1.2 Novelty of This Work

To the best of our knowledge, there are two approaches to find the optimality of deployment patterns. One is to compute the lower bound of Voronoi size for a particular k and then to prove that a proposed pattern has the same Voronoi size as the lower bound [8]–[14]. This approach is used to obtain the optimal pattern for k-connectivity. The second approach is to compute the pattern such that the overlapping area by sensor nodes is minimized [1], [5], which is used to obtain the optimal 1, 2, and 3-coverage patterns.

Thus, the existing works prove the optimality of deployment patterns for individual k one by one. However, our approach is totally different. The novelty of this paper lies a recursive algorithm to obtain the optimal deployment pattern for different k values that achieves the k-coverage condition.

1.3 Organization

The rest of this paper is organized as follows: In Section 2, the terms Voronoi region and regular tessellations are introduced. In Section 3, an efficient algorithm which finds the optimal k-coverage deployment pattern for any k value is provided. In Section 4, the optimal deployment patterns for $4 \leq k \leq 9$ are identified using our proposed algorithm. Performances of the proposed deployment patterns are evaluated in Section 5. Related works are reviewed in Section 6. Section 7 concludes this paper and provides the future directions of this research.

2 Preliminary

2.1 Voronoi Diagrams

Given a set of n point sites $V = \{v_1, \ldots, v_n\}$, its Voronoi diagram partitions the 2-D plane into n Voronoi cells, each contains exactly one point site. The Voronoi cell of a point site is defined as the collection of points closer or equal to the site than any other site. The boundary of a Voronoi cell is always composed by line segments, straight lines, and/or half lines. The Voronoi cell of a point site includes its borders and vertices, which consist of all points in the 2-D plain that are equivalent to two or more nearest sites, respectively.

2.2 Tessellations

A *tessellation* of a two dimensional plane is a decomposition of the plane by the pattern that fills the plane without overlapping or gap. Each piece of the pattern in a tessellation is called a *tessella*, and a tessellation is said to be *regular* if all of its tessellae are equiangular and equilateral, such as triangle, square, pentagon, hexagon, and so forth. First, we introduce Theorem 1 without the proof. The readers interested in the proof can refer to [15].

Theorem 1 *There exist exactly three regular tessellations (triangle, square, and hexagon) in a 2-D plane, which are shown in Figure 1 (a), (b), and (c), respectively.*

According to Theorem 1, there exist only three regular tessellations. In other words, a collection of other regular patterns that are equiangular and equilateral, such as pentagons, heptagons, octagons, and so on, cannot fill a plane without overlapping or gap.

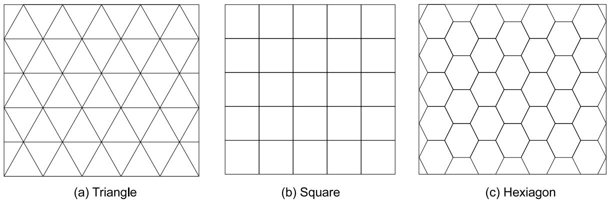
(a) Triangle (b) Square (c) Hexiagon

Fig. 1. Regular tessellations.

A *semi-regular* tessellation is composed of more than one kind of regular tessellae. For instance, Trihexagonal semi-regular tessellation consists of triangle and hexagon tessellae as shown in Figure 2 (a). There exist eight such semi-regular tessellations [16]. However, they cannot represent a Voronoi diagram according to Theorem 2.

Theorem 2 *None of the semi-regular tessellations can represent a Voronoi diagram.*

Proof: We will prove the above claim by contradiction. Assume any of the semi-regular tessellations represents a Voronoi diagram. If a tessellation represents a Voronoi diagram, each tessella contains a node at its center, and two neighboring tessellae share an edge with the same distance to their node. However, all the semi-regular tessellations consist of two or more tessellae with different polygons. For two neighboring regular tessella, the distances between the center of them and the shared edge must be different. This is a contradiction. Therefore, the claim must be true. □

For example, Figure 2 (b) depicts the two neighboring polygons in the Trihexagonal pattern. It is clear that the distance between v_0 and a point on the line $\overline{A_0A_1}$ is shorter than the distance between v_1 and the point. Thus, the Trihexagonal pattern does not represent a Voronoi diagram. Similar argument holds for all other semi-regular tessellations.

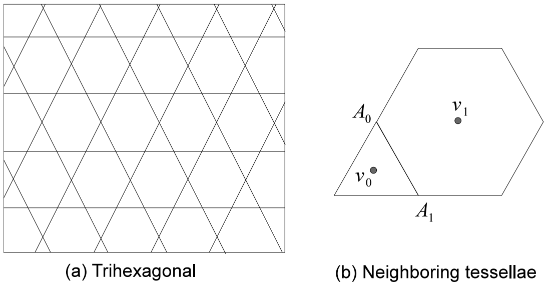

(a) Trihexagonal (b) Neighboring tessellae

Fig. 2. Trihexagonal tiling pattern.

Theorem 2 implies that no semi-regular pattern can be the Voronoi diagram of the optimal deployment pattern. Therefore, in the following sections, we consider only regular tessellations.

2.3 Problem Formulation, Definitions and Assumptions

The k-coverage deployment is used for wireless sensor networks and RFID applications. The deployed entities, such as wireless sensors and RF tags, are referred to as $nodes$. The k-coverage deployment problem is defined as finding a deployment pattern such that every point in the region is covered by at least k nodes. In other words, every point in the region is covered by at least one node even when $k-1$ nodes are removed from the network. Unlike the k-connectivity deployment problem, we are not concerned about the connectivity among nodes, and therefore, the communication range of nodes is ignored. (Note that for our purpose the communication range between RFID tags and readers is considered as the sensing range for tags.) Nevertheless, in most cases the wireless graph constructed by the proposed k deployment pattern is connected, since the node density is high. In this paper, our goal is to find the k-coverage deployment patterns which minimize the number of deployed nodes.

Due to the simplicity of deployment and the requirement of applications, the deployment pattern is always symmetric and tends to repeat itself. When nodes are deployed in such a fashion, the Voronoi diagram of the deployed nodes will naturally be a regular tessellation if the boundary of the deployed region is not considered. Because of the nature of symmetry, the shape of the Voronoi cell for a node in such a situation can only be one of the known regular tessellae. Figure 3 (a), (b), and (c) illustrate three regular patterns, where a circle represents a node and the area surrounded by solid lines represents a tessella. From Figure 3 (b), we can easily derive that the square pattern is formed by square tessellae. However, the tessellae in the triangle pattern is formed by hexagon tessellae, as shown in Figure 3 (a), while the tessellae in the hexagon pattern are triangles as depicted in Figure 3 (c). Therefore, there are three regular deployment patterns, the triangle, the square, and the hexagon patterns, each of which is considered as a collection of hexagon, square, and triangle tessellae, respectively.

The distance between two nearest deployed nodes is denoted as d^*. Note that the actual tessella size cannot be computed without knowing d^*, but each closed regular pattern always has the unique tessella polygon. For clarification, we explicitly denote a tessella T given a closed regular pattern, and the tessella size $|T|$ as the size of tessella with a given d^* of the regular pattern. Therefore, an optimal deployment can be determined if its tessella polygon and d^* are given. As can be seen in Figure 3, the side length of each tessella polygon has a linear relationship to d^*. For a given d^*, the tessella sizes for the aforementioned patterns are shown in Table 1.

Also, we define *subtessella* by a subarea of a tessella as shown by bold lines in Figure 4. Let N_n be the number of the nearest neighbors. Each tessella is composed of N_n identical subtessellae. Due to the symmetric nature, if one of the subtessellae is k-covered, the tessella is k-covered.

The notations utilized in this paper are summarized in Table 2.

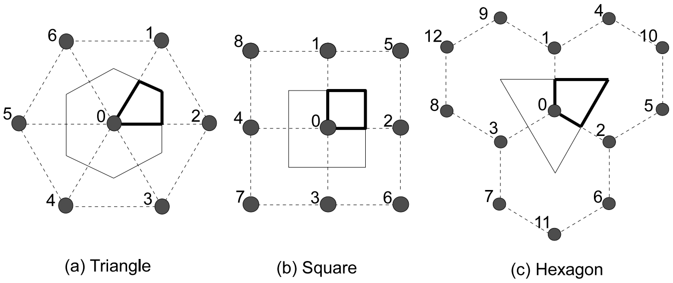

(a) Triangle (b) Square (c) Hexagon

Fig. 4. Subtessella of each tessellation.

3 The Framework

3.1 A Naive Approach

At the first glance, it seems to be natural that the optimal k-coverage deployment can be achieved by deploying k number

TABLE 1
Equations to obtain the tessellation sizes.

Regular pattern	Tessellation size
Square	d^{*2}
Triangle	$\frac{\sqrt{3}}{2}d^{*2}$
Hexagon	$\frac{3\sqrt{3}}{4}d^{*2}$

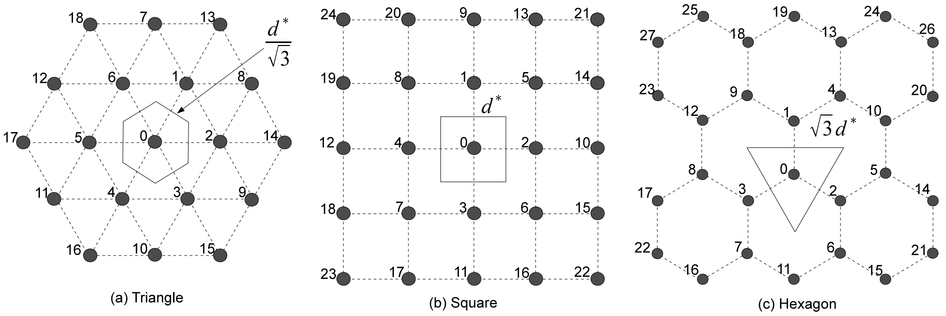

(a) Triangle (b) Square (c) Hexagon

Fig. 3. Tessellae for each deployment pattern.

TABLE 2
Notations.

Symbol	Definition
V	The set of all nodes in the region
v_i	Node v_i
r	The radius of coverage area
k	The number of coverage
C_i	The area of circle centered by v_i
$d(i,j)$	The distance between two points i and j
$D(p,a)$	The distance range between a point p and an area a
L_t	The sorted list for an area t
$L_t(i)$	The set of nodes in the i-th L_t
d^*	The distance of the closest neighbors
N_n	The number of nearest nodes
T	A tessella
$\|T\|$	Tessella size
t	A subtessella
R_t	The radius of the circum circle of t
o_t	The center of the circum circle of t
$DL(i,t)$	The distance between a node in $L_t(i)$ and o_t.
Pt	A regular pattern $\{tri, sq, hex\}$
$DP(k,Pt,d^*)$	The deployment pattern for given k, Pt, and d^*

of the optimal 1-coverage pattern for the same region. While this strategy is not guaranteed to create regular patterns, the optimal 2-coverage pattern (the hexagon pattern with $d^* = r$) and the optimal 3-coverage pattern (the triangle pattern with $d^* = r$) can indeed be constructed by overlapping 2 and 3 of the optimal 1-coverage pattern (the triangle pattern with $d^* = \sqrt{3}r$), respectively. To be specific, in Figure 5 (a), the set of black nodes distanced by $\sqrt{3}r$ form one triangle pattern, and the rest of the nodes (i.e., the set of white nodes) form another triangle pattern. Each of these sets is exactly one optimal 1-coverage pattern. The combination of these two sets forms a hexagon pattern, where the closest pair of a black and a white node have distance r. The hexagon pattern is known as the optimal 2-coverage pattern [5]. Similarly, in Figure 5 (b), there are three types of nodes: the nodes colored by black, the nodes colored by white, and the rest colored by grey. Each set of nodes with the same color is one optimal 1-coverage pattern, and the combination of these three sets forms the optimal 3-coverage triangle pattern with $d^* = r$ [5].

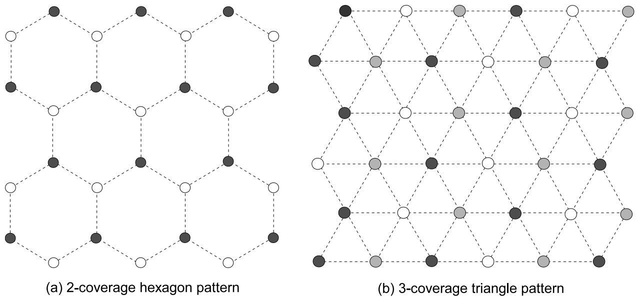

(a) 2-coverage hexagon pattern (b) 3-coverage triangle pattern

Fig. 5. The optimal coverage for $k = 2, 3$.

From the above observation, it seems that the optimal k-coverage pattern can be constructed by overlapping k optimal 1-coverage patterns. Unfortunately, this approach does not work for $k \geq 4$ because as we will demonstrate in the following sections, there are patterns to achieve k-coverage with fewer nodes.

3.2 The Basic Idea

A sensor network can be deployed either randomly or manually. When a sensor network is deployed randomly, sensor nodes are assumed to be placed in the region in a randomized fashion. For instance, sensors can be dropped from an airplane to a remote and hard-to-access area [17], [18]. In such type of deployment, it is important to know the critical density which guarantees certain properties [19]–[21]. However, when a sensor network is deployed in a building or factory, sensor nodes will be deployed either manually or by robots. In such type of deployment, it is natural for the deployment pattern to be regular and symmetric for the following reasons:

- When sensor nodes are deployed in a regular and symmetric pattern, the distance between any pair of closest neighbors will be the same. For a wireless application, this allows a single version of the algorithm to be run at every node. If irregular patterns are used for deployment, application designers have to handle many different cases depending on the location of a node due to the lack of symmetry.

- Irregular deployment patterns imply that the deployment can not be processed by a simple robot and consequently will increase the cost of network deployment significantly.

When the deployment pattern is regular and symmetric, except the area close to the boundary, the Voronoi cell (i.e., tessella) associated with each node should have the same shape and size. Hence, finding the optimal pattern under a given k-coverage requirement is equivalent to finding the pattern that maximizes the size of the tessella [10]. According to Theorem 1, there exist only three regular tessellations for a 2-D plane. If each closed Voronoi cell has the same shape, the deployment pattern has to be one of these regular tessellations. This confines our search to only these regular tessellae for the optimal k-coverage deployment pattern. Based on this idea, we are able to develop a framework to efficiently identify the optimal pattern for a given coverage requirement.

3.3 Range Elimination Scheme

Let $d(p_1, p_2)$ be the Euclidean distance between p_1 and p_2, the *distance range* between a node v_i and a subtessella t is defined as $D(v_i, t) = \{d(v_i, p) : \forall p \in t\}$. Between two distance ranges, we define $D(v_i, t) < D(v_j, t)$ if $\forall p \in t$, $d(v_i, p) < d(v_j, p)$, and $D(v_i, t) \lesssim D(v_j, t)$ if $\forall p \in t$, $d(v_i, p) \leq d(v_j, p)$. In addition, we denote $D(v_i, t) \sim D(v_j, t)$ if there exist $p_m, p_n \in t$, $d(v_i, p_m) < d(v_j, p_m)$ and $d(v_i, p_n) > d(v_j, p_n)$. For example, let t be the subtessella that refers to the upper right of the tessella centered by v_0 in Figure 3 (b). Then, we will have $D(v_0, t) < D(v_{14}, t)$, $D(v_1, t) \sim D(v_2, t)$, and $D(v_0, t) \lesssim D(v_1, t)$.

Given a subtessella t, consider the minimum circum circle that encloses t. The radius and the center of the circum circle are denoted as R_t and o_t, respectively. We can sort all nodes based on their distance from o_t. Let L_t be such a sorted list. In this list, the i-th element is denoted as $L_t(i)$. Note that $L_t(i)$ contains a set of nodes that have the same distance to o_t, and $|L_t(i)| \geq 1$. Clearly, $L_t(i) \cap L_t(j) = \emptyset$ when $i \neq j$ and the list contains all the nodes in the deployment area, i.e., $\bigcup_{i=0}^{\infty} L_t(i) = V$. We denote $d_l(t)$ and $d_u(t)$ the lower bound and the upper bound of the distance range between a node and a subtessella t, respectively. Let $DL(i, t)$ be the distance between o_t and a node in $L_t(i)$. To eliminate nodes from the consideration of k-coverage, we derive Theorem 3.

Theorem 3 *Given a subtessella t, nodes with $d_l(t) > DL(k, t) + R_t$ are never used to cover t in the optimal k-coverage deployment pattern.*

Proof: The k-th nearest node has the distance $DL(k, t)$ to the subtessella t and its $d_u(t)$ is less than or equal to $DL(k, t) + R_t$. Thus, if the sensing circle of any node with its $d_l(t) > DL(k, t) + R_t$ intersects at any point of the subtessella t, the sensing circle of any k-th nearest node contains the subtesella t. When the sensing circle of the k-th nearest nodes encloses t, the subtessella is already k-covered. Thus, the optimal deployment pattern never contains nodes with $d_l(t) > DL(k, t) + R_t$ to cover t. This concludes the proof. □

Figure 6 illustrates the example of Theorem 3 for the square pattern for $k = 3$. The list L_t will be $\{v_0\}$, $\{v_1, v_2\}$, $\{v_5\}$, $\{v_3, v_4\}$, $\{v_6, v_8\}$, $\{v_7\}$, $\{v_9, v_{10}\}$, and so on. $R_t = \frac{\sqrt{2}}{4} d^*$ and $R_3 = d(v_5, o_t) = \frac{3\sqrt{2}}{4} d^*$. For node v_{10}, its $d_l = \frac{3}{2} d^*$. Thus, $d_l(t) > R_t + DL(3, t)$. This indicates when the sensing circle C_{10} intersects any point in t, the circle C_5 already contains t. Since v_5 is in $L_t(3)$, t is 3-covered when C_5 contains t. Therefore, v_{10} is excluded from the consideration of the optimal 3-coverage for t. Similarly, we can eliminate all nodes in $L_t(i)$ for $i \geq 7$. Thus, Theorem 3 implies that only a finite set of nodes in the network needs to be scanned to obtain the optimal k-coverage deployment pattern.

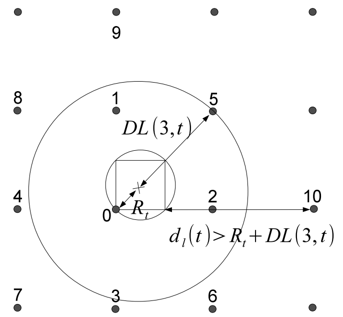

Fig. 6. Range elimination.

Next, we will elaborate on the framework to discover the optimal k-coverage deployment pattern. We first need to know the subtessella t, which is shown in Figure 4. Then, we will sort nodes based on the distance to o_t, which is also unique to a given regular pattern and a subtessella regardless of the value of k.

Note that all R_t and $DL(i, t)$, and all $d_l(t)$ and $d_u(t)$ for each node have a linear relationship with the distance between the nearest neighbors, d^*. After eliminating unnecessary nodes to k-cover t based on Theorem 3, the list will contain a finite number of nodes. The set of these nodes is denoted as S_k. We will scan the power set of S_k. For each subset of S_k denoted by S, we check the following three conditions:

- **Condition 1 -** For any pair of $v_i, v_j \in S$, either $D(v_i, t) \lesssim D(v_j, t)$, $D(v_j, t) \lesssim D(v_i, t)$, or $D(v_i, t) \sim D(v_j, t)$ holds.
- **Condition 2 -** For any $v_i \in S$, v_i has $k - 1$ nodes, say v_j, such that $D(v_j, t) \lesssim D(v_i, t)$.
- **Condition 3 -** The union of the sensing circles C_i of $v_i \in S$ encloses t.

Among the subset of nodes S that satisfies the above conditions, we choose one with the longest distance between nearest neighbors.

Computing the power set of S_k can be done more efficiently with the recursive nature of our RES. Let CS_{k-1} be the set of nodes that cover t for the optimal $(k-1)$-coverage, then CS_k must contain CS_{k-1} as we deduce the following Lemma. Note that for any k, CS_k is a subset of S_k since the optimal pattern is obtained by scanning nodes in S_k.

Lemma 4 *$CS_{k-1} \subset CS_k$ holds, where CS_k is the set of nodes providing the optimal k-coverage for a subtessella t.*

Proof: The proof is by contradiction. If the claim were false, there must exist a node with $d_l(t) < DL(k-1,t) + R_t$ but $d_l(t) > DL(k,t) + R_t$. The sorted list L_t is total order. Thus, $DL(i,t) > DL(j,t)$ for any $i > j$, and such a node does not exist, which is a contradiction. This concludes the proof. □

Lemma 4 indicates that our RES is recursive, and only the subsets of S_k that contains CS_{k-1} need to be considered for the optimal k-coverage pattern.

The skeleton of our algorithm is given in Algorithm 1. We first call $FindOptimalDeployment(k)$, which is defined from line 1 to 13 in Algorithm 1. Since the calculation of the distance of two closest nodes is different for each k and each regular pattern Pt, for every k and Pt we run RES defined by $RangeEliminationScheme(k, Pt)$ from line 16 to 34. By comparing the tessellation size obtained from Table 1 with the distance derived from RES, we can identify the optimal deployment pattern.

Algorithm 1 The skeleton of RES.

```
1: FindOptimalDeployment($k$)
2: $SIZE_{max} \leftarrow 0$
3: $DP_{opt} \leftarrow null$
4: for each regular pattern, $Pt \in \{tri, sq, hex\}$ do
5:     $DP \leftarrow RangeEliminationScheme(k, Pt)$
6:     /* $DP.size$ is tessella size */
7:     compute $DP.size$ by Table 1 with $DP.d^*$
8:     if $DP.size > SIZE_{max}$ then
9:         $SIZE_{max} \leftarrow DP.size$
10:        $DP_{opt} \leftarrow DP$
11:    end if
12: end for
13: return $DP_{opt}$
14:
15: /* RES */
16: RangeEliminationScheme($k$, $Pt$)
17: $d_{max} \leftarrow 0$
18: $Pt_{max} \leftarrow null$
19: /* for any node $i$, do the following */
20: compute $t$ from $T$ and $Pt$
21: compute $L_t$ from $L_t(1)$ to $L_t(k+c)$ where $c$ is a constant relatively
    much larger than $k$.
22: compute $R_i$ for a node in each $L_t(i)$ $1 \leq i \leq k$.
23: compute a set $S_k$ by eliminating nodes from $L_t$ by Theorem 3
24: for each subset $S$ of $S_k$, where $S$ contains $CS_{k-1}$ (Lemma 4) do
25:     if $S$ satisfies all condition 1, 2, and 3 then
26:         compute $d^*$ from the relative location of $v_i \in S$
27:         if $d^* > d_{max}$ then
28:             compute $|T|$ from Table 1 with $d^*$
29:             $d_{max} \leftarrow d^*$
30:             $Pt_{max} \leftarrow Pt$
31:         end if
32:     end if
33: end for
34: return $DP(k, Pt_{max}, d_{max})$.
```

3.4 The Correctness of RES

In this subsection, we prove that Range Elimination Scheme can successfully identify the optimal k-coverage deployment pattern.

Theorem 5 *Given a regular pattern Pt and k, the deployment which results in the maximum edge length of the closed Voronoi cell (i.e., tessella) for interior nodes and covers a subtesella t forms the optimal k-coverage deployment pattern.*

Proof: First, if the deployment pattern is regular, the Voronoi cell of nodes in the interior of the deployment region must form a regular tessellation. Let d^* be the distance between nearest neighbors to guarantee that the subtessella t is covered k times. On the one hand, it is clear that if we enlarge d^*, the subtessella is not k-covered. On the other hand, from Table 1, we can see that the size of the tessella is proportional to the d^*, and it monotonically decreases as d^* decreases. Thus, making d^* shorter will result in a smaller tessella, which will lead to more nodes deployed in the given region. Therefore, the claim is true. □

Theorem 5 tells us how to obtain the *optimal* size for a given regular pattern. However, to find the optimal deployment pattern, we must search and compare the results of all regular patterns. This is why we run RES on all three regular patterns in Algorithm 1.

Next we show that the running time of RES is $O(2^k)$ regardless of the input size, i.e., the number of nodes in the deployment region.

Lemma 6 $\sum_{i=0}^{k} |L_t(i)|$ *is upper bounded by $O(k)$.*

Proof: Let N_n be the number of nearest neighbors for any node. From Figure 3, it is clear that $N_n = 6$ for the triangle pattern, which has hexagon tessellae; $N_n = 4$ for the square pattern, which has square tessellae; and $N_n = 3$ for the hexagon pattern, which has triangle tessellae. We can see that N_n equals the number of subtessellae. To compute $|L_t(i)|$, without loss of generality, let us consider the right upper subtessella t in the triangle pattern in Figure 4 (a). The number of nodes with the same distance to v_0 inside of the angle $\angle v_1 v_0 v_2$ is a constant c. As each subtessella contains the same number of nodes, $|L_t(i)|$ is linear to c. There are two cases to compute $|L_t(i)|$.

Case 1 (Inclusive): In this case, some nodes in $L_t(i)$ are on the lines extended from $\overline{v_0 v_1}$ and $\overline{v_0 v_2}$. Since neighboring subtessellae share the nodes on these lines, $|L_t(i)| = (c-2)N_n + N_n = (c-1)N_n$.

Case 2 (Exclusive): In this case, some nodes in $L_t(i)$ are on the lines extended from $\overline{v_0 v_1}$ and $\overline{v_0 v_2}$. No other subtessella shares any of these nodes, and therefore $|L_t(i)| = cN_n$.

Hence, $|L_t(i)| \leq cN_n$ for any $i \geq 0$. Therefore, $\sum_{i=0}^{k} |L_t(i)| \leq ckN_n = O(k)$. This concludes the proof. □

Lemma 7 *For a given k value, the set of nodes S_k scanned by RES is bounded by $O(k)$.*

Proof: . Since S_k is obtained by scanning L_t from the head, there must be the index $k+c$ where c is a constant such that $S_k \subset \bigcup_{i=0}^{k+c}$. From Lemma 6, we can deduce $|S_k|$ is bounded by $O(k+c)$, and thus $O(k)$. Therefore, the claim must be true. □

Lemma 6 proves that we need to scan a constant number of nodes for a given k value and a regular pattern.

Theorem 8 *Given a regular pattern and k, RES always terminates in $O(2^k)$.*

Proof: Each regular pattern has a unique tessella T and identical subareas t. Since the sensing range of each node is constant, the distance between two nodes for 1-coverage deployment pattern must be a constant. This indicates that t is always a finite area for any given k. From Lemma 7, the nodes that could be in S_k can be found in constant time. As all possible subsets are obtained from the power set of S_k, there are $O(2^k)$ possible subsets to consider.

For each subset, we need to check if the subset satisfies the three conditions and calculate the corresponding distance between the nearest nodes d^*. This computation can be done in constant time. Therefore, the algorithm terminates in $O(2^k)$. This concludes the proof. □

Although the time complexity of our algorithm is exponential, the value of k is normally small. For instance, very few applications require more than 6-coverage. In addition, the optimal deployment pattern is usually computed offline before the deployment actually takes place. Therefore, the performance of our RES is acceptable in real applications.

4 Optimal Deployment Patterns

The proposed RES successfully discovers the optimal pattern for arbitrary k. Due to the space constraint, we do not elaborate on how RES works for $1 \leq k \leq 3$. In this section, we will demonstrate RES for $4 \leq k \leq 9$.

In the following, we assume node IDs are assigned to each node in increasing order by distance from an arbitrary node, i.e. v_0, and in clockwise order. The ID assignment for each regular pattern is shown in Figure 3. In addition, we say T is the tessella of node v_0. The subarea of the tessella t refers to the upper right subtessella of node v_0 for all regular patterns as shown in Figure 4 (a), (b), and (c), respectively.

Theorem 9 *The square pattern with $d^* = \frac{4}{5}r$ achieves the optimal 4-coverage.*

Proof: Consider three nodes v_3, v_4, and v_5. Condition 1 is met, because they have the same distance range to t. Each of v_3, v_4, and v_5 has the distance range to t larger than three nodes. For example, $D(v_0,t)$, $D(v_1,t)$, $D(v_2,t) < D(v_3,t)$. This satisfies condition 2. Clearly, condition 3 holds. As shown in Figure 7, the nearest neighbors' distance d^* is maximized when C_3, C_4, and C_5 intersect at $p \in t$. Note that all v_3, v_4, and v_5 have the same distance range to t, and so there always exists such a point p. Let A_0 be the middle point of the line $\overline{v_3v_4}$. The points A_0, p, and v_e form a perpendicular triangle. Since $d(p,v_3) = r$ and $d(A_0,v_3) = \frac{1}{\sqrt{2}}d_e$, we can obtain:

$$\begin{aligned} d(v_5,A_0) &= d(v_5,p) + d(p,A_0) & (1)\\ \frac{3\sqrt{2}}{2}d^* &= r + \sqrt{r^2 - (\frac{1}{\sqrt{2}}d^*)^2} & (2)\end{aligned}$$

Therefore, when $d^* = \frac{3\sqrt{2}}{5}r$, every point in the region is covered four times. Similarly, we can derive d^* for the triangle and hexagon patterns. The Voronoi size of the square pattern with $d^* = \frac{3\sqrt{2}}{5}r$ is larger than that of the triangle and hexagon patterns. This completes the proof. □

Note that CS_4 for the square pattern contains all v_i for $1 \leq i \leq 6$, since they provide coverage for t.

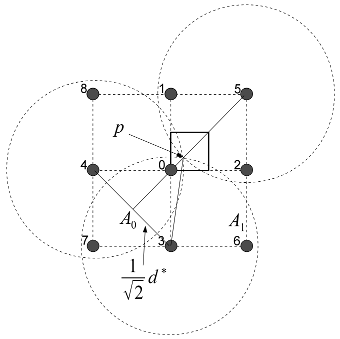

Fig. 7. The pattern for $k = 4$.

The upper bound of tessella size created by overlapping the optimal 1-coverage pattern four times is $\frac{1}{4} \cdot \frac{\sqrt{3}}{2}d^{*2} \simeq 0.645r^2$ by Table 1. However, the square pattern with the edge length $\frac{3\sqrt{2}}{5}r$ results in larger tessella size of $0.72r^2$. Hence, the square pattern with $d^* = \frac{3\sqrt{2}}{5}r$ requires a lower number of nodes compared with overlapping the optimal 1-coverage pattern four times. This shows that overlapping the optimal 1-coverage pattern k times does not result in the optimal k-coverage deployment pattern.

Theorem 10 *The equilateral triangle pattern with $d^* = \frac{2}{\sqrt{7}}r$ achieves the optimal 5-coverage.*

Proof: The above claim is proved in a similar fashion as Theorem 9, and so we briefly show the proof. The subset $\{v_4, v_6, v_8, v_9\}$ satisfies the three conditions, and d^* is maximized when C_4, C_6, C_8, and C_9 intersect at p in Figure 8. Clearly, $d(v_1,v_6) = d^*$, and $d(v_1,p) = \frac{\sqrt{3}}{2}d^*$ since p is the middle point between v_0 and v_2. For C_6 to intersect at p, the distance between v_6 and p must be r. Thus, Equation 3 is established and we can compute d^* as follows.

$$\begin{aligned} d(v_6,p) &= \sqrt{d(v_1,v_6)^2 + d(v_1,p)^2} & (3)\\ &= \sqrt{d^{*2} + (\frac{\sqrt{3}}{2}d^*)^2} & (4)\end{aligned}$$

We want to let $d(v_6,p)$ be r. Thus, the triangle pattern with $d^* = \frac{2}{\sqrt{7}}r$ provides 5-coverage. Among the Voronoi size of all regular patterns, the triangle pattern with $d^* = \frac{2}{\sqrt{7}}r$ is the optimal 5-coverage pattern. This concludes the proof. □

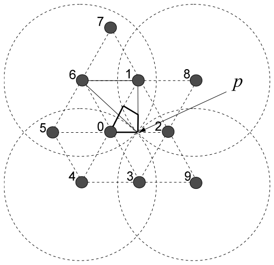

Fig. 8. The pattern for $k = 5$.

Theorem 11 *The equilateral triangle pattern with $d^* = \frac{5}{7}r$ achieves the optimal 6-coverage.*

Proof: The set of nodes v_5, v_8, and v_9 satisfies the three conditions, and d^* for the optimal pattern is obtained as follows. Figure 9 (a) depicts the intersection point p of C_5, C_8, and C_9. Let A_0 be a point on the line $\overline{v_4 v_9}$ such that $\angle pA_0v_9$ is $\frac{1}{2}\pi$, and A_1 be a point on the line $\overline{v_4 v_9}$ such that $\angle v_0A_1v_9$ is $\frac{1}{2}\pi$. It is clear that $d(p, v_9) = r$ and $d(p, A_0) = \frac{\sqrt{3}}{2}d^*$. Also, $d(A_0, v_9) = d(A_1, v_9) - d(A_1, A_0)$. Since $d(v_0, p) = d(A_1, A_0)$ and $d(v_5, p) = r$, we can say $d(A_1, A_0) = r - d^*$ and $d(A_0, v_9) = \frac{3}{2}d^* - (r - \frac{3}{2}d^*) = \frac{5}{2}d^* - r$. Hence, we can derive:

$$\begin{aligned} d(p, v_9) &= \sqrt{d(p, A_0)^2 + d(A_0, v_9)^2} && (5) \\ r^2 &= (\frac{\sqrt{3}}{2}d^*)^2 + (\frac{5}{2}d^* - r)^2 && (6) \end{aligned}$$

Hence, $d^* = \frac{5}{7}r$. Comparing the Voronoi size of the other regular patterns, we can deduce that the triangle pattern with $d^* = \frac{5}{7}r$ achieves the optimal 6-coverage. This concludes the proof. □

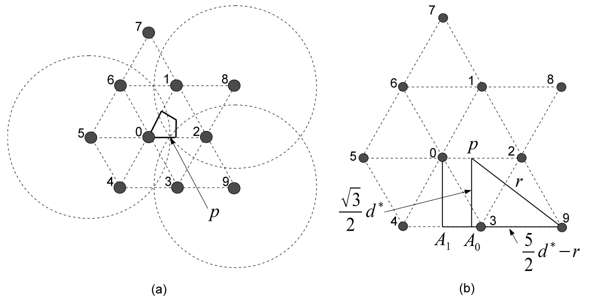

Fig. 9. The pattern for $k = 6$.

Theorem 12 *The square pattern with $d^* = \sqrt{2/5}r$ achieves the optimal 7-coverage.*

Proof: A set of nodes v_6 and v_8 satisfies the three conditions. Let p in Figure 10 be the center point of nodes v_0, v_1, v_2, and v_5. When C_6 and C_8 intersect at point p, the sub-tessella is 7-covered. Let A_0 be the center point on the line $\overline{v_3 v_6}$. From Figure 10, it is clear that $d(A_0, v_6) = \frac{1}{2}d^*$ and $d(p, A_0) = \frac{3}{2}d^*$. Thus, we can deduce $d^* = \sqrt{2/5}r$.

With this result, the square pattern has the largest Voroni size among regular patterns. Therefore, the square pattern with $d^* = \sqrt{2/5}r$ achieves the optimal 7-coverage. This concludes the proof. □

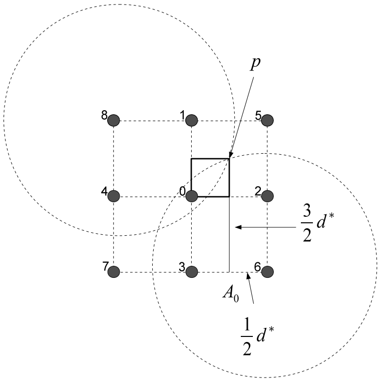

Fig. 10. The pattern for $k = 7$.

Theorem 13 *The square pattern with $d^* = \frac{3}{5}r$ achieves the optimal 8-coverage.*

Proof: A set of nodes v_7, v_9, and v_{10} satisfies the three conditions. When C_7 and C_9 (or C_7 and C_{10}) intersect on the line $\overline{v_0, v_1}$ (or $\overline{v_0, v_2}$) as shown in Figure 11, the sub-tessella is 8-covered. Let p be such a point on the line $\overline{v_0, v_1}$. Let δ be the distance between v_0 and p. Then, we will have two equations as follows.

$$\delta + r = 2d^* \qquad (7)$$

$$r^2 = d^{*2} + (d^* + \delta)^2 \qquad (8)$$

By computing Equation 7 and 8, we can deduce $d^* = \frac{3}{5}r$. Considering the Voronoi size obtained by other regular patterns, the square pattern with $d^* = \frac{3}{5}r$ achieves the optimal 8-coverage. This concludes the proof. □

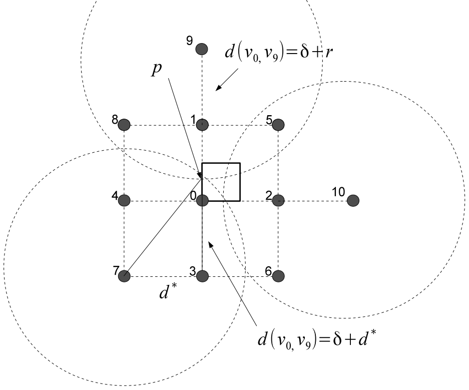

Fig. 11. The pattern for $k = 8$.

Theorem 14 *The hexagon pattern with* $d^* = \sqrt{3/13}r$ *achieves the optimal 9-coverage.*

Proof: A set of nodes v_6 and v_8 satisfies the three conditions. When C_6 and C_8 intersects at point p in Figure 12, the sub-tessella is 9-covered. Let A_0 and A_2 be the center point of the line $\overline{v_8 v_{12}}$ and $\overline{v_5 v_{10}}$, then p is somewhere on the line $\overline{A_0 A_2}$. Let A_1 be the center point of the line $\overline{v_0 v_1}$, and we define δ as $d(A_1, p)$. We have $d(A_0, A_1) = \sqrt{3}d^* + \delta d^*$ and $d(v_8, A_0) = \frac{1}{2}d^*$. From the triangle with vertices v_8, A_0, and p, we can deduce Equation 9.

$$(\sqrt{3}d^* + \delta d^*)^2 + (\frac{1}{2}d^*)^2 = r^2 \tag{9}$$

Let A_3 be a point on the line $\overline{v_6 v_7}$, and the line $\overline{pA_3}$ is perpendicular to $\overline{v_6 v_7}$. Since $d(v_6, A_3) = \frac{\sqrt{3}}{2}d^* - \delta d^*$ and $d(p, A_3) = 2d^*$, Equation 10 can be obtained.

$$(\frac{\sqrt{3}}{2}d^* - \delta d^*)^2 + (2d^*)^2 = r^2 \tag{10}$$

From Equation 9 and 10, we can compute $d^* = \sqrt{3/13}r$. Comparing Voronoi size obtained by other regular patterns, we can conclude that the triangle pattern with $d^* = \sqrt{3/13}r$ results in the optimal 9-coverage. This completes the proof. □

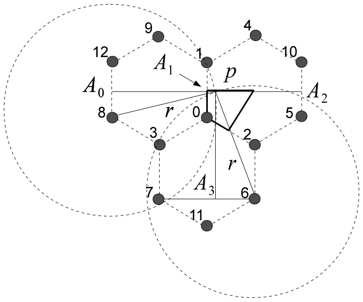

Fig. 12. The pattern for $k = 9$.

Remark Note that for a given regular pattern, it is possible that k-coverage and $(k+1)$-coverage deployment patterns result in the same d^*. For instance, all of the optimal 5-coverage, 6-coverage, 7-coverage square deployment patterns have the same nearest neighbors' distance, $\sqrt{2/5}r$, as shown in Table 3. In other words, the problem of finding the optimal 7-coverage deployment pattern for the square regular pattern contains that of finding the optimal 5-coverage and 6-coverage deployments for the same pattern.

5 Performance Evaluation

In this section, we evaluate the performance of the three regular patterns. Our performance evaluation includes both analytical and simulation results.

TABLE 3
The deployment pattern for each k. The optimal patterns are shown by boldface font.

k	Square	Triangle	Hexagon
1	$\sqrt{2}r$	$\sqrt{\mathbf{3}}\mathbf{r}$ [7]	r
2	r	r	$\mathbf{r}$ [5]
3	$\frac{2}{\sqrt{5}}r$	$\mathbf{r}$ [5]	$\frac{2}{\sqrt{7}}r$
4	$\mathbf{\frac{3\sqrt{2}}{5}r}$	$\frac{\sqrt{3}}{2}r$	$\frac{5}{7}r$
5	$\sqrt{2/5}r$	$\mathbf{\frac{2}{\sqrt{7}}r}$	$\frac{1}{\sqrt{3}}r$
6	$\sqrt{2/5}r$	$\mathbf{\frac{5}{7}r}$	$\frac{1}{\sqrt{3}}r$
7	$\sqrt{\mathbf{2/5}}\mathbf{r}$	$\frac{2}{3}r$	$\frac{1}{2}r$
8	$\mathbf{3/5r}$	$\frac{1}{\sqrt{3}}r$	$\frac{1}{2}r$
9	$\frac{2}{\sqrt{17}}r$	$\frac{1}{\sqrt{3}}r$	$\sqrt{\mathbf{3/13}}\mathbf{r}$

5.1 Analytical Results

The tessella size of regular patterns is used to evaluate deployment patterns for theoretical aspects. Table 3 shows that the maximal d^* to achieve k-coverage for each regular pattern. The optimal pattern for each regular tessellation is marked by bold font. Recall that given a deployment pattern and d^*, we can compute the tessella size by Table 1. In addition, we compared the optimal patterns with the square pattern since it is the most used deployment pattern. The relative tessella size is defined by the ratio between the performance of the optimal pattern given a regular pattern and the performance of the square pattern.

Figure 13 illustrates the tessella size with respect to the value of k for different deployment patterns. It seems that when $k \geq 3$, the deployment patterns result in similar performance. However, a small difference in one tessella becomes a large difference as the number of nodes to be deployed increases. Thus, the optimal deployment pattern significantly reduces the cost of node deployment.

Figure 14 presents the tessella size (1st y-axis on the left) and ratio between the optimal pattern and square patterns (2nd y-axis on the right) with respect to the value of k. Note that the square pattern is optimal when $k = 4, 7, 8$; hence, the relative tessella size is 1 for $k = 4, 7, 8$. From the figure, we can see that the optimal pattern achieves up to 25% larger tessella size compared with the square pattern.

5.2 Simulation Results

We have conducted simulations to evaluate the performance of the deployment patterns, including the triangle, the square, and the hexagon patterns. In our simulation, nodes are deployed in

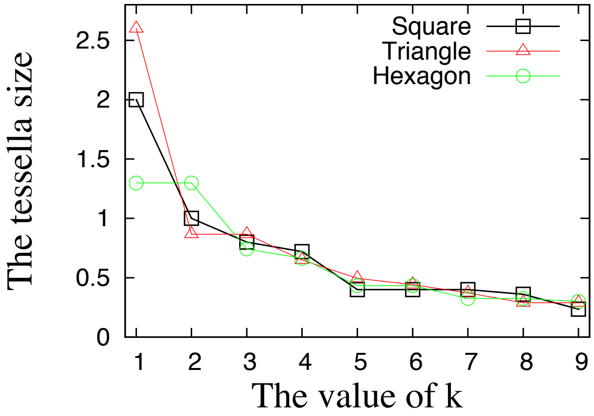

Fig. 13. The performance of deployment patterns.

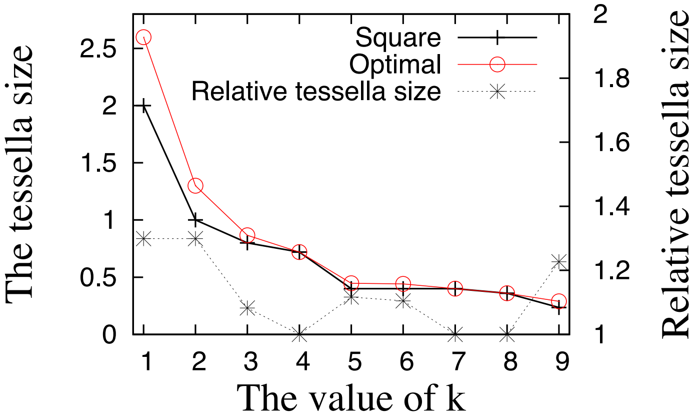

Fig. 14. The tessella size and relative tessella size of deployment patterns.

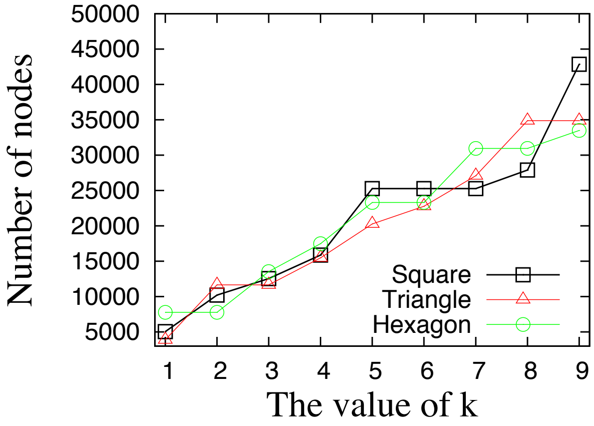

Fig. 15. The number of deployed nodes.

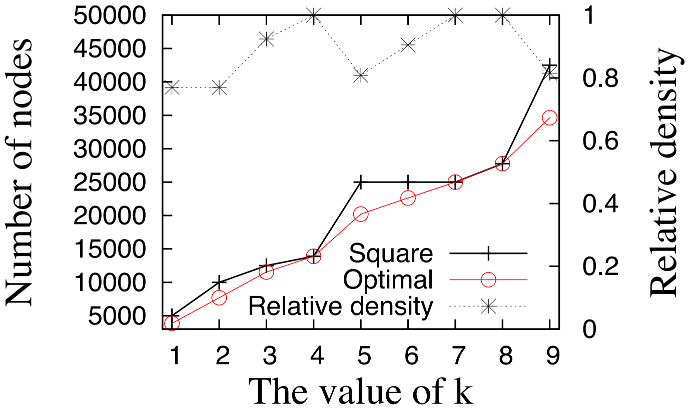

Fig. 16. The number of deployed nodes.

the 100 by 100 square region with the sensing range of 1 unit. We use node density as a metric to evaluate the performance, which is defined by the number of nodes per unit disk (the sensing area). In addition, we calculate the relative density with respect to the square pattern, since the square pattern is the most intuitive and easiest to deploy. The relative density is defined by the number of nodes required by the optimal pattern divided by the number required by the square pattern.

Figure 15 demonstrates the number of nodes with respect to the value of k for different deployment patterns. When $k \geq 5$, the difference among deployment patterns is up to 9000 nodes. Considering both Figure 13 and 15, the deployment pattern plays a very important role.

Figure 16 depicts the number of nodes (1st y-axis on the left) and relative density (2nd y-axis on the right) with respect to the value of k for the optimal and square patterns. From the figure, when $k = 5, 6, 9$, the optimal pattern requires only 80% to 90% of nodes required by the square pattern to cover every point in the region k times. Again, when $k = 4, 7, 8$, the square pattern is the optimal pattern, therefore the relative density is 1.

5.3 Comparison between Analysis and Simulation

To validate our analysis, we conducted the brute force algorithm for three regular patterns. Given a tessella size, d^* is calculated by Table 1, and then we check the achievable k values (the number of coverage) that a deployment pattern provides. Figure 17 shows the achievable k values with respect to the given tessella size. For example, the line for the square pattern (the dotted line) goes up to 4 in the y-axis when the tessella size is 0.72. This implies that the square pattern is optimal when $k = 4$. When the tessella size is 0.72, d^* is $\sqrt{0.72} \approx 0.848 \approx \frac{3\sqrt{2}}{5}$. This matches to d^* discussed in Table 3. Similarly, we validate the results of our RES in Table 3 and the simulation results.

5.4 Comparison with Probabilistic Random Deployment

We compared the deployment patterns found by RES with the random deployment. In the random deployment, sensor nodes are randomly deployed in a region. Starting with the minimum number of sensor nodes, a set of sensor nodes are added until the deployment pattern satisfies a given coverage requirement. Since the complete k-coverage of a region by the random

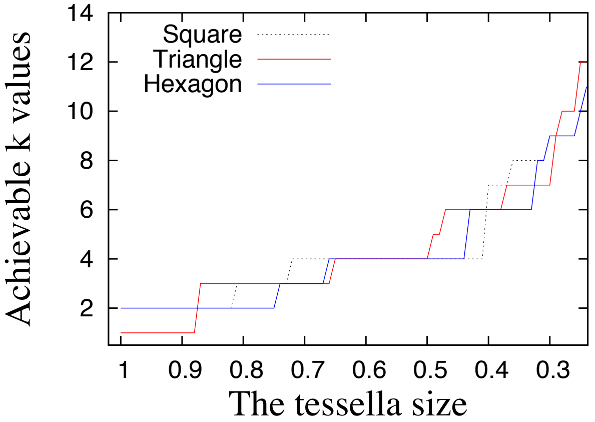

Fig. 17. Achievable k value under different tessella sizes.

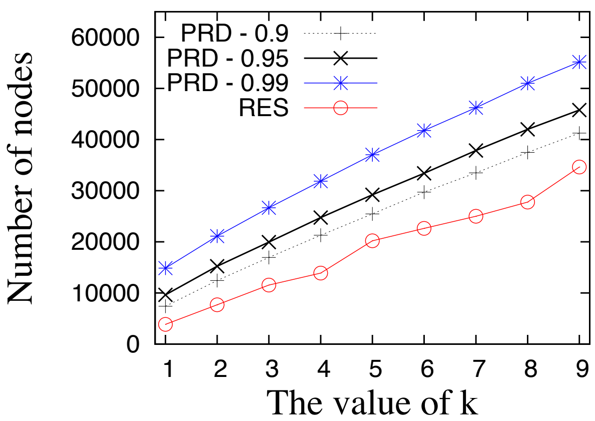

Fig. 18. Comparison with the random deployment.

deployment is too expensive, we introduce the probabilistic random deployment (PRD) that guarantees p percent of the region are covered by at least k nodes. We denote such a scheme by PRD-p. To be specific, PRD-0.9, PRD-0.95, and PRD-0.99 are implemented in the simulation. The simulation setting is the same as that described in Section 5.2.

Figure 18 shows the number of nodes required by the deployment patterns found by our RES and PRD-p ($p = \{0.9, 0.95, 0.99\}$). As can be seen from the figure, the required nodes to provide k-coverage increases as the the value of k increases. Since the proposed RES results in the optimal pattern, our scheme always requires the minimum number of sensor nodes and provides the 100% of k-coverage when compared with PRD-p. From Figure 18, we can conclude that the optimal pattern found by RES helps deploy sensors efficiently to provide the complete k-coverage.

6 Literature Review

The circle covering problem was first introduced by Kershner [7] in 1939. It has been shown that the equilateral triangle pattern with $d^* = \sqrt{3}r$, where r is the radius of circle that each node can cover, is the optimal pattern to cover a given region with the minimum number of circles. When it comes to wireless applications, such as wireless sensing [1], RFID sensing [4], activity monitoring [2], localization [5], barrier coverage [22], [23] and so on, it is important to consider both k-connectivity and k-coverage. In wireless sensing applications, sensor nodes need to be deployed so that they can communicate with each other in keeping with the full coverage. To improve the robustness of sensor networks, k-connectivity is a preferred property, where each pair of nodes has k independent paths between them. The higher connectivity a sensor network is, the more fault-tolerant to nodal failure or crash the system is.

In addition, the importance of k-coverage deployments can be observed in localization applications [5]. Assume deployed nodes in a region have their location, and every point in the region is covered by at least k nodes. The deployed nodes with location information can be used as reference points to localize an intruder. Obviously, a higher k-coverage results in more accurate localization.

6.1 k-Connectivity Deployments

The k-connectivity deployment problem is to find a deployment pattern such that the graph is k-connected with the minimum number of nodes. k-connectivity deployment patterns are typically used for wireless sensing. Two critical parameters, the communication range and the the sensing range, need to be considered. In [8]–[11], Bai et al. identified and proved the optimal deployment patterns for various ratios of the communication and sensing range for $k \leq 6$.

6.2 k-Coverage Deployments

k-coverage deployment problem is to find a deployment pattern such that every point in the region is covered by at least k nodes with the minimum number of nodes. When $k = 1$, it is the same as the circle covering problem [7], and the equilateral triangle pattern with the nearest neighbors' distance $d^* = \sqrt{3}r$ is optimal. In [5], Ku et al. proved that the hexagon pattern with $d^* = r$ is optimal for $k = 2$, and the equilateral triangle pattern with $d^* = r$ is optimal for $k = 3$. Note that in [5] the authors claim that the diamond pattern with $d^* = r$ is optimal for $k = 3$, but it is the same as the equilateral triangle with $d^* = r$ if we see the pattern from a different angle. In [24], Bai *et al.* further identified the optimal 2-coverage deployment patterns under different ratios of the communication and sensing range.

The optimal k-coverage deployment pattern has various applications. One example is barrier coverage [22], [23]. In k-coverage deployment, monitoring area is covered even if $k-1$ of sensors fail. As a result, the barrier will be more invulnerable and reliable. Other examples are indoor localization [5] and vehicle localization [25], where sensors or RFID tags are deployed on the ground as reference points to locate a robot or vehicle. One of the realizations is KIVA Systems [26], which is an automatic inventory management used by Amazon.com Inc. The results presented in [5] demonstrates that localization accuracy improves as k increases.

6.3 Deployment with Practical Setting

Recent works consider sensor deployment problems with practical setting, such as the connected coverage with directional antennas [27] and the deployment pattern in bounded area [28].

7 Conclusion and Future Work

The optimal deployment pattern drastically reduces the number of nodes to be deployed and operational cost in wireless network applications. In this paper, we propose Range Elimination Scheme (RES) to discover the optimal k-coverage deployment pattern for arbitrary k values. We demonstrate how RES identifies the optimal k-coverage deployment pattern for $4 \leq k \leq 9$. The analytical and simulation results validate that the proposed algorithm successfully discovers the optimal deployment pattern for the given k value. Moreover, our simulation results indicate that the optimal pattern significantly reduces node deployment costs for large scale wireless network applications.

The proposed framework can be extended to various deployment optimization problems. For instance, when the deployment pattern is symmetric, the optimal multiple connectivity and coverage deployment patterns for 2-D networks can be identified using a similar algorithm. In addition, when the deployment pattern is symmetric, the deployment optimization problems for 3-D space can also be treated as a 3-D regular tessellation. We plan to study these problems by extending our framework.

References

[1] H. Zhang and J. Hou, "Maintaining Sensing Coverage and Connectivity in Large Sensor Networks," *Ad Hoc and Sensor Wireless Networks*, vol. 1, no. 1-2, pp. 89–124, 2005.

[2] Y. Liu, L. Chen, P. Jian, Q. Chen, and Y. Zhao, "Mining Frequent Trajectory Patterns for Activity Monitoring Using Radio Frequency Tag Arrays," in *PerCom*, 2007, pp. 37–46.

[3] J. Teng, J. Zhu, B. Zhang, D. Xuan, and Y. F. Zheng, "E-V: Efficient Visual Surveillance with Electronic Footprints," in *Infocom*, 2012, pp. 109–117.

[4] L. M. Ni, Y. Liu, Y. C. Lau, and A. P. Patil, "Landmarc: Indoor location sensing using active rfid," in *PerCom*, 2003, pp. 407–415.

[5] W.-S. Ku, K. Sakai, and M.-T. Sun, "The Optimal k-Covering Tag Deployment for RFID-based Localization," *Journal of Network and Computer Applications*, vol. 34, no. 3, pp. 914–924, 2011.

[6] M. Li, Z. Li, and A. V. Vasilakos, "A Survey on Topology Control in Wireless Sensor Networks: Taxonomy, Comparative Study, and Open Issues," *Proceedings of the IEEE*, vol. 101, no. 12, pp. 2538–2557, 2013.

[7] R. Kershner, "The Number of Circles Covering a Set," *American Journal of Mathmatics*, vol. 61, pp. 665–671, 1939.

[8] X. Bai, S. Kumar, D. Xuan, Z. Yun, and T.-H. Lai, "Deploying Wireless Sensors to Achieve both Coverage and Connectivity," in *Mobihoc*, 2006, pp. 131–142.

[9] X. Bai, D. Xuan, Z. Yun, T.-H. Lai, and W. Jia, "Complete Optimal Deployment Patterns for Full-Coverage and k-Connectivity (k<=6) Wireless Sensor Networks," in *Mobihoc*, 2008, pp. 401–410.

[10] X. Bai, Z. Yun, D. X. T. H. Lai, and W. Jia, "Optimal Patterns for Four-connectivity and Full Coverage in Wireless Sensor Networks," *IEEE Transactions on Mobile Computing*, vol. 9, no. 3, pp. 435–448, 2010.

[11] X. Bai, Z. Yun, D. Xuan, W. Jia, and W. Zhao, "Pattern Mutation in Wireless Sensor Deployment," in *Infocom*, 2010, pp. 2480–2488.

[12] S. M. N. Alam and Z. J. Haas, "Coverage and Connectivity in Three-Dimensional Networks," in *Mobicom*, 2006, pp. 346–357.

[13] X. Bai, C. Zhang, D. Xuan, and W. Jia, "Full-Coverage and k-Connectivity (k=14, 6) Three Dimensional Networks," in *Infocom*, 2009, pp. 388–396.

[14] X. Bai, C. Zhang, D. Xuan, J. Teng, and W. Jia, "Low-Connectivity and Full-Coverage Three Dimensional Wireless Sensor Networks," in *Mobihoc*, 2009, pp. 145–154.

[15] J. Britton, *Symmetry and Tesselations: Investination Patterns*. Dale Seymour Publications, 1999.

[16] MathWorld, "Semi-regular tessellations,"
http://mathworld.wolfram.com/SemiregularTessellation.html.

[17] U. Berkeley and M. Co, http://www-bsac.eecs.berkeley.edu/ pister/29Palms0103/.

[18] A. Saipulla, B. Liu, and J. Wang, "Barrier Coverage with Airdropped Sensors," in *MILCOM*, 2008.

[19] P.-J. Wan, C.-W. Yi, and L. Wang, "Asymptotic Critical Transmission Radius for k-Connectivity in Wireless Ad Hoc Networks," *IEEE Transactions on Information Theory*, vol. 56, pp. 2867–2874, 2010.

[20] M. D. Penrose, "On k-Connectivity for a Geometric Random Graph," *Random Structures Algorithm*, vol. 15, pp. 145–164, 1999.

[21] P.-J. Wan and C.-W. Yi, "Coverage by Randomly Deployed Wireless Sensor Networks," *IEEE /ACM Transactions on Networking*, vol. 14, pp. 2658–2669, 2006.

[22] S. Kumar, T.-H. Lai, and A. Arora, "Barrier Coverage with Wireless Sensors," in *Mobicom*, 2005, pp. 284–298.

[23] A. Chen, S. Kumar, and T.-H. Lai, "Designing Localized Algorithms for Barrier Coverage," in *Mobicom*, 2007, pp. 63–74.

[24] X. Bai, Z. Yun, D. Xuan, B. Chen, and W. Zhao, "Optimal Multiple-Coverage of Sensor Networks," in *Infocom*, 2011, pp. 2264–2272.

[25] W. Cheng, X. Cheng, M. Song, B. Chen, and W. W. Zhao, "On the Design and Deployment of RFID Assisted Navigation Systems for VANETs," *TPDS*, vol. 23, no. 7, pp. 1267–1274, 2012.

[26] KIVA Systems LLC. http://www.kivasystems.com/.

[27] Z. Yu, J. Teng, X. Bai, D. Xuan, and W. Jia, "Connected Coverage in Wireless Networks with Directional Antennas," in *Infocom*, 2011, pp. 2264–2272.

[28] Z. Yu, J. Teng, X. Li, D. Xuan, and W. Jia, "On Wireless Network Coverage in Bounded Areas," in *Infocom*, 2013, pp. 1195–1203.

Kazuya Sakai (S'09-M'14) received his Ph.D. degree in Computer Science and Engineering from The Ohio State University in 2013. Since 2014, he has been an assistant professor at the Department of Information and Communication Systems, Tokyo Metropolitan University. His research interests are in the area of wireless networks, mobile computing, and network security. He is a member of the IEEE.

Min-Te Sun (S'99-M'02) received his B.S. degree in mathematics from National Taiwan University in 1991, the M.S. degree in computer science from Indiana University in 1995, and the Ph.D. degree in computer and information science from the Ohio State University in 2002. Since 2008, he has been with Department of Computer Science and Information Engineering at National Central University, Taiwan. His research interests include distributed algorithm design and wireless network protocol development.

Wei-Shinn Ku (S'02-M'07-SM'12) received his Ph.D. degree in Computer Science from the University of Southern California (USC) in 2007. He also obtained both the M.S. degree in Computer Science and the M.S. degree in Electrical Engineering from USC in 2003 and 2006, respectively. He is an associate professor with the Department of Computer Science and Software Engineering at Auburn University. His research interests include spatial data management, mobile data management, geographic information systems, and security and privacy. He has published more than 70 research papers in refereed international journals and conference proceedings. He is a senior member of the IEEE.

Ten H. Lai Ten H. Lai is a Professor of Computer Science and Engineering at the Ohio State University. He is interested in applying Zen to teaching and research. He served as program chair of ICPP 1998, general chair of ICPP 2000, program co-chair of ICDCS 2004, general chair of ICDCS 2005, and recently, general co-chair of ICPP 2007. He is/was an editor of IEEE Transactions on Parallel and Distributed Systems, ACM/Springer Wireless Networks, Academia Sinica's Journal of Information Science and Engineering, International Journal of Sensor Networks, and International Journal of Ad Hoc and Ubiquitous Computing.

Athanasios V. Vasilakos is currently Professor at the University of Western Macedonia, Greece. He has authored or coauthored over 200 technical papers in major international journals and conferences. He is author/coauthor of five books and 20 book chapters in the areas of communications. Prof. Vasilakos has served as General Chair, Technical Program Committee Chair, TPC member (i.e INFOCOM, SECON, MOBIHOC) for many international conferences. He served or is serving as an Editor or/and Guest Editor for many technical journals, such as the IEEE TNSM, IEEE TIFS, IEEE TSMC PartB, IEEE TITB, IEEE TC, ACM TAAS, the IEEE JSAC special issues of May 2009, Jan 2011, March 2011, the IEEE Communications Magazine, ACM/Springer WINET, ACM/Springer MONET. He is founding Editor-in-Chief of IJAACS and IJART. He is also General Chair of the Council of Computing of the European Alliances for Innovation.